TURBULENT DISPERSION IN STABLY STRATIFIED SHEAR FLOW

Frank G. Jacobitz
Department of Mechanical Engineering
University of California, Riverside
Riverside, California 92521-0425, USA
jacobitz@engr.ucr.edu

ABSTRACT

Direct numerical simulations are performed in order to investigate turbulent dispersion of concentration fields in stably stratified shear flow. The Richardson number is varied from $Ri = 0$, corresponding to unstratified shear flow, to $Ri = 0.4$, corresponding to strongly stratified shear flow. The total energy is found to grow for weakly stratified cases with $Ri \leq 0.1$ and to decay for strongly stratified cases with $Ri > 0.1$. The kinetic energy is distributed unevenly over the three velocity components with *downstream* > *spanwise* > *vertical*.

Turbulent dispersion of two species c_z and c_y with initially Gaussian mean concentration variations in the vertical z and spanwise y directions is investigated. At a given Richardson number Ri, a slower spreading of c_z in the vertical direction is observed compared to the spreading of c_y in the spanwise direction. This observation is consistent with a lower turbulent fluctuation level in the vertical velocity component compared to the spanwise velocity component. With increasing Richardson number, dispersion in both the vertical and spanwise direction is decreased due to decreased turbulent velocity fluctuations. A variation of the initial widths of the mean concentration profiles results in nearly identical values of the widths toward the end of the simulations.

INTRODUCTION

Understanding of turbulent dispersion of substances released into the geophysical environment is incomplete. For example, two conflicting dispersion models have been proposed in the past and are widely used to parameterize vertical dispersion of pollutants in the atmospheric boundary layer (Hunt 1982; Venkatram, Strimaitis and Dicristofaro 1984). The turbulent motion in the geophysical environment is strongly affected by the competing effects of shear and density stratification. In this study, direct numerical simulations are performed in order to study turbulent dispersion in stably stratified shear flow.

The prototypical example of stably stratified shear flow with uniform vertical shear and uniform vertical stable stratification is considered here. In this flow, the mean downstream velocity component and the mean density vary linearly in the vertical direction:

$$U = Sz \qquad V = W = 0 \qquad \varrho = \rho_0 + S_\rho z \qquad (1)$$

The shear rate $S = \partial U/\partial z$ and the stratification rate $S_\rho = \partial \varrho/\partial z$ are constant.

Due to its geophysical importance, stably stratified shear flow has been studied extensively in the past. Using energy considerations, Richardson (1920) and Taylor (1931) established the Richardson number $Ri = N^2/S^2$ as the primary parameter to describe the stability of stratified shear flow. Here, $N = \sqrt{-gS_\rho/\rho_0}$ is the Brunt-Väisälä frequency and S is the shear rate. Miles (1961) and Howard (1961) showed that the flow is stable for $Ri > 1/4$ using linear inviscid stability analysis. More recently, stably stratified shear flow has been studied in great detail, both experimentally (Komori, Ueda, Ogino and Mizushina 1983; Rohr, Itsweire, Helland and Van Atta 1988; Piccirillo and Van Atta 1997), as well as numerically (Gerz, Schumann and Elghobashi 1989; Holt, Koseff and Ferziger 1992; Itsweire, Koseff, Briggs and Ferziger 1993; Jacobitz, Sarkar and Van Atta 1997; Jacobitz 2000).

In the simulations performed here, two scalar concentration fields c_z and c_y are present. Both species fields initially have a Gaussian mean concentration variation with a maximum in the center of the computational domain. The mean of c_z varies in the vertical z direction and the mean of c_y varies in the spanwise y direction. This allows the study of both vertical and spanwise turbulent dispersion in stably stratified shear flow.

In the following section, the numerical approach is summarized. Then, the evolution of the flow field is addressed and the dispersion of the species fields is discussed. Finally, the observations of the current study are summarized.

NUMERICAL APPROACH

The direct numerical simulations performed here are based on the continuity equation for an incompressible fluid, the unsteady three-dimensional Navier-Stokes equation in the Boussinesq approximation, and advection-diffusion equations for the density and concentration fields. In the direct numerical approach, all dynamically important scales of the velocity, density, and concentration fields are resolved. The equations are solved in a frame of reference moving with the mean flow (Rogallo 1981). A spectral collocation method is used for the spatial discretization and the solution is advanced in time with a fourth-order Runge-Kutta scheme. All simulations are initialized with an isotropic turbulence field that was allowed to evolve for about one eddy-turnover time in a separate simulation without shear or stratification. Initially, there are no density or concentration fluctuations present. The simulations are performed on a parallel computer using a grid with up to $256 \times 256 \times 256$ points.

RESULTS

In this section, results from a series of direct numerical simulations are presented, in which the Richardson number is varied from $Ri = 0$ to $Ri = 0.4$. All simulations are initialized with isotropic turbulence fields without density or concentration fluctuations. The initial Taylor microscale Reynolds number $Re_\lambda = 45$ and the initial shear number

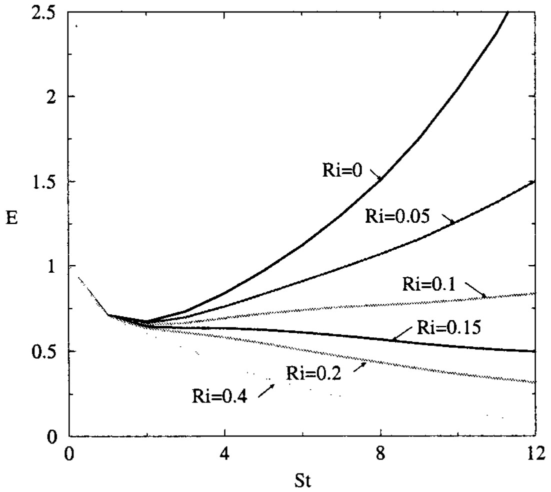

Figure 1: Evolution of the total energy E with nondimensional time St. The Richardson number is varied from $Ri = 0$ (unstratified shear flow) to $Ri = 0.4$ (strongly stratified shear flow).

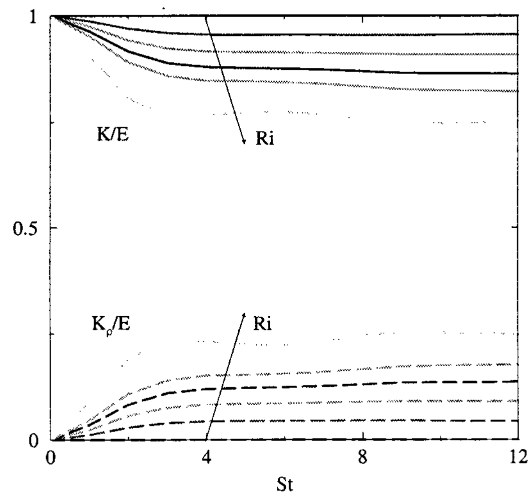

Figure 2: Evolution of the energy partition K/E (solid lines) and K_ρ/E (dashed lines) with nondimensional time St. The arrows indicate an increase of the Richardson number from $Ri = 0$ to $Ri = 0.4$.

$SK/\epsilon = 2$ are matched in all cases. The Reynolds number reaches values as high as $Re_\lambda = 100$ and the shear number assumes a value $SK/\epsilon = 6$ in the simulations. The Prandtl number of the density field is $Pr = 0.7$ and the Schmidt number of the concentration fields is $Sc = 2$. The species fields c_z and c_y initially have a Gaussian-shaped mean concentration variation in the vertical z and spanwise y direction, respectively. In the following, the energetics of the velocity and density fields are presented first. Then the evolution of the concentration fields is discussed.

Energetics

Figure 1 shows the evolution of the total energy $E = K + K_\rho$ with nondimensional time St. Here $K = \overline{u_i u_i}/2$ is the turbulent kinetic energy and $K_\rho = g\overline{\rho\rho}/(2\rho_0 S_\rho)$ is the potential energy. Initially, the total energy E decays due to the isotropic initial conditions until the shear production of turbulence develops at about $St = 3$. For strongly stratified cases with Richardson numbers $Ri > 0.1$, the total energy E continues to decay. For weakly stratified cases with $Ri \leq 0.1$, the total energy E eventually grows as the simulations advance in time.

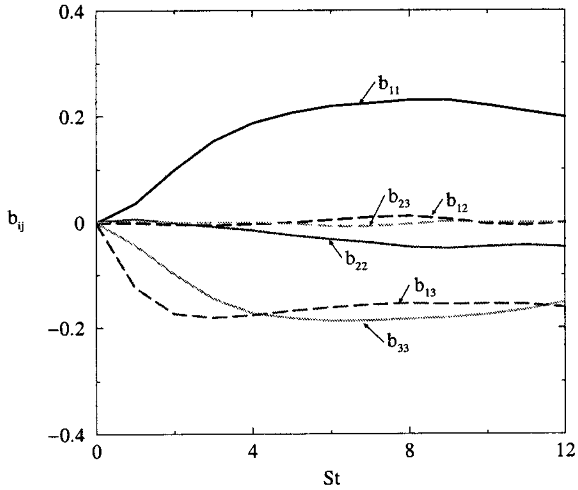

Figure 3: Evolution of the diagonal (solid lines) and off-diagonal (dashed lines) components of the Reynolds stress anisotropy tensor b_{ij} with nondimensional time St. The Richardson number is $Ri = 0$.

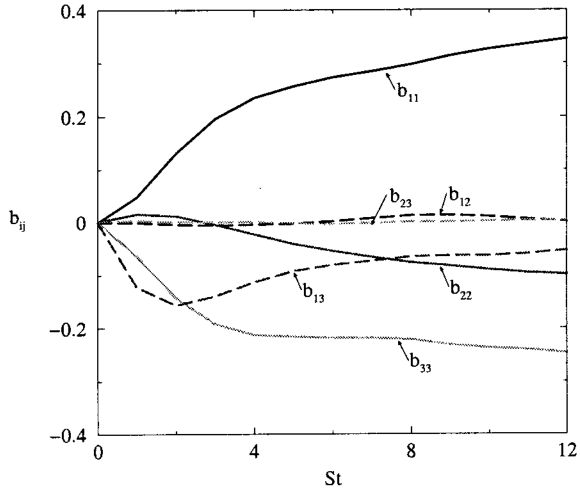

Figure 4: Evolution of the diagonal (solid lines) and off-diagonal (dashed lines) components of the Reynolds stress anisotropy tensor b_{ij} with nondimensional time St. The Richardson number is $Ri = 0.2$.

Figure 2 shows the contribution of the turbulent kinetic energy to the total energy K/E (solid lines) and the contribution of the potential energy to the total energy K_ρ/E (dashed lines). As the Richardson number Ri is increased, the contribution of the potential energy K_ρ/E increases, while the contribution of the turbulent kinetic energy K/E decreases. The strongly stratified case with $Ri = 0.4$ shows a periodic exchange between kinetic and potential energy, indicating the presence of internal waves in the flow field.

In order to evaluate the distribution of the turbulent kinetic energy over the three velocity components, the Reynolds stress anisotropy tensor b_{ij} is considered:

$$b_{ij} = \frac{\overline{u_i u_j}}{\overline{u_k u_k}} - \frac{1}{3}\delta_{ij} \qquad (2)$$

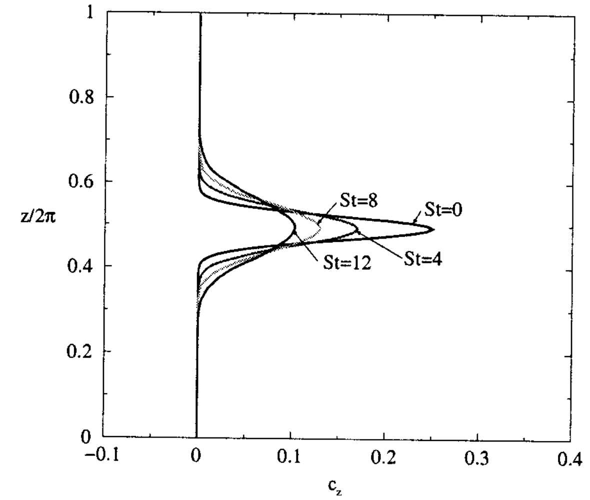

Figure 5: Evolution of the vertical mean concentration field c_z with nondimensional time St. The Richardson number is $Ri = 0$.

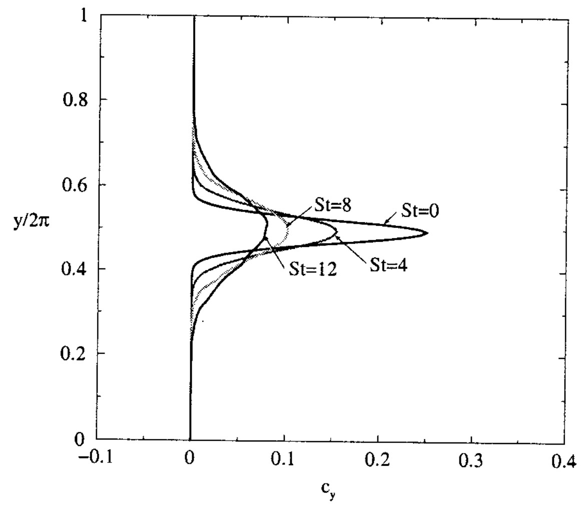

Figure 6: Evolution of the horizontal mean concentration field c_y with nondimensional time St. The Richardson number is $Ri = 0$.

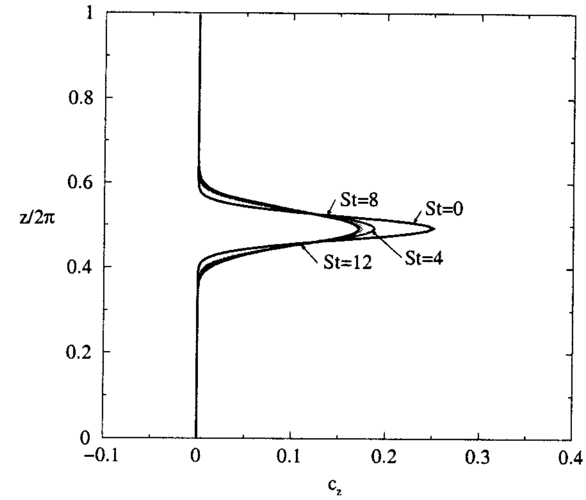

Figure 7: Evolution of the vertical mean concentration field c_z with nondimensional time St. The Richardson number is $Ri = 0.2$.

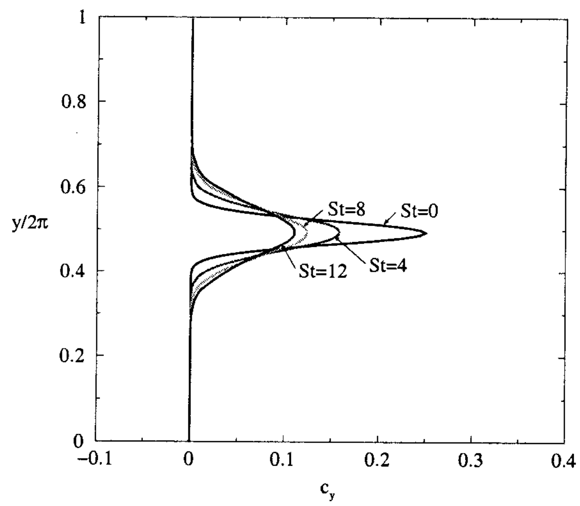

Figure 8: Evolution of the horizontal mean concentration field c_y with nondimensional time St. The Richardson number is $Ri = 0.2$.

Note that all components of b_{ij} vanish for isotropic turbulence.

Figure 3 shows the evolution of the components of the Reynolds stress anisotropy tensor b_{ij} for an unstratified simulation with $Ri = 0$. The solid lines show the diagonal components of the tensor. Due to shear production of turbulence, b_{11} has a surplus. The kinetic energy K is distributed over the three velocity components with *downstream* > *spanwise* > *vertical*. The dashed lines show the off-diagonal components of b_{ij}. Due to the symmetry of the problem only the b_{13} component is nonzero. This component is directly related to the normalized production of turbulence (Jacobitz *et al.* 1997).

Figure 4 shows the evolution of the components of the Reynolds stress anisotropy tensor b_{ij} for a strongly stratified simulation with $Ri = 0.2$. As in the unstratified case with $Ri = 0$, the kinetic energy K is distributed over the velocity components with *downstream* > *spanwise* > *vertical*. The level of anisotropy, however, is increased. The b_{33} component has a larger deficit due to the conversion of vertical kinetic energy to potential energy. Also, the magnitude of the b_{13} component is decreased, indicating a reduced production of kinetic energy in the strongly stratified case.

Turbulent Dispersion

In this section, the dispersion of the concentration fields c_z and c_y is discussed. The species field c_z initially has a Gaussian mean concentration variation in the vertical z direction and the species field c_y initially has a Gaussian mean concentration variation in the spanwise y direction. The maximum concentration of both species is located in the center of the computational domain. Both concentration fields are initialized without concentration fluctuations.

Figures 5 and 6 show the evolution of the mean concentration variation of c_z and c_y, respectively, for an unstratified simulation with $Ri = 0$. The mean concentration components are obtained from plane averages in the vertical z direction of c_z and from plane averages in the spanwise y direction of c_y. As the simulation advances in nondimensional time St, the mean profiles decay in amplitude and disperse considerably. Consistent with the observation that the spanwise velocity component is more energetic that the

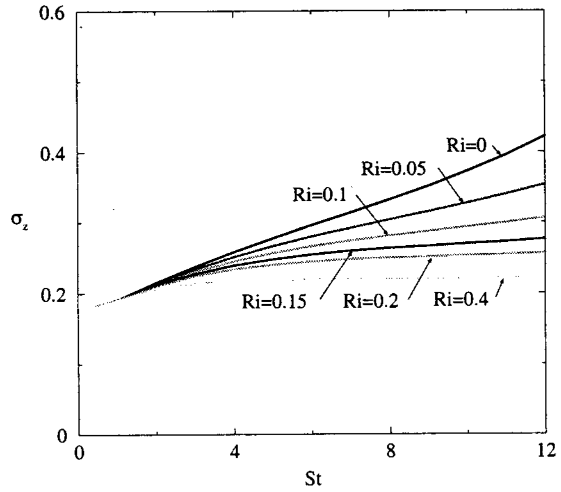

Figure 9: Evolution of the width σ_z with nondimensional time St. The Richardson number is varied from $Ri = 0$ to $Ri = 0.4$.

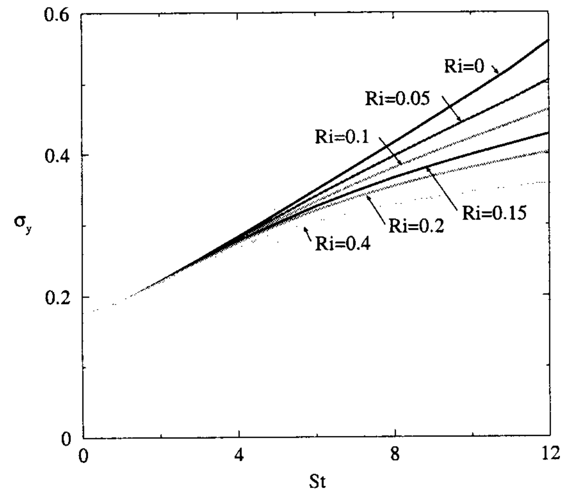

Figure 10: Evolution of the width σ_y with nondimensional time St. The Richardson number is varied from $Ri = 0$ to $Ri = 0.4$.

vertical velocity component, the spread of c_y in the spanwise direction is stronger that the spread of c_z in the vertical direction. Similarly, the decay of the maximum mean concentration is more rapid for c_y than for c_z.

Figures 7 and 8 show the evolution of the mean concentration variation of c_z and c_y, respectively, for a strongly stratified simulation with $Ri = 0.2$. Again, the spanwise spread of c_y is stronger that the vertical spread of c_z. The maximum mean concentration of c_y decays much more rapidly than the maximum mean concentration of c_z.

A comparison between the unstratified and stratified cases shows that the decreased turbulence levels of the stratified case leads to decreased dispersion rates in the spanwise direction and, particularly, the in the vertical direction.

A good measure for the vertical extend of the concentration field c_z is given by σ_z:

$$\sigma_z^2 = \frac{\int c_z (z - z_0)^2 dz}{\int c_z dz} \tag{3}$$

Similarly, the spanwise extend of the concentration field c_y can be determined by σ_y:

$$\sigma_y^2 = \frac{\int c_y (y - y_0)^2 dy}{\int c_y dy} \tag{4}$$

Here, z_0 and y_0 denote the positions of the maximum mean concentration.

Figures 9 and 10 show the evolution of σ_z and σ_y, respectively, for all simulations performed here with Richardson numbers from $Ri = 0$ to $Ri = 0.4$. Initial spreading of the concentration fields is observed for all cases due to the isotropic turbulence with which the simulations are started.

The vertical spreading of c_z is strongest for the unstratified case with $Ri = 0$, in which σ_z reaches about twice its initial value at the end of the simulation at $St = 12$. The vertical spreading is reduced with increasing Richardson number Ri as the vertical turbulent kinetic energy decreases. The strongly stratified case with $Ri = 0.4$ shows nearly no spreading after the initial decay of the turbulent velocity fluctuations.

The spanwise spreading of c_y again is strongest for the unstratified case. Here, σ_y reaches about three times its initial value at the end of the simulation at $St = 12$. With increasing Richardson number Ri the spreading of c_y decreases. Due to the higher fluctuation level in the spanwise velocity component, compared to the vertical velocity component, the spanwise spreading is always stronger than the vertical spreading at a given Richardson number.

Figures 11 and 12 show the evolution of the concentration fluctuations c'_z and c'_y, respectively, for the unstratified simulation with $Ri = 0$. The concentration fluctuations are obtained as plane averages in the vertical z direction of c'_z and from plane averages in the spanwise y direction of c'_y. The simulations are initialized without concentration fluctuations. Concentration fluctuations develop quickly and show a maximum close to the regions of maximum mean concentration gradient. A decay of the concentration fluctuation magnitude is observed as a result of the competing effects of decaying mean concentrations and increasing velocity fluctuations. As the vertical velocity component has a lower fluctuation level than the spanwise velocity component, the mean concentration spreads more slowly in the vertical direction. Therefore, the mean concentration gradient remains larger in the vertical direction, resulting in a higher level of concentration fluctuations.

Figures 13 and 14 show the evolution of the concentration fluctuations c'_z and c'_y, respectively, for a strongly stratified simulation with $Ri = 0.2$. Here, the vertical velocity component is suppressed by stratification, resulting a a lower concentration fluctuation level of c'_z compared to c'_y.

Figures 15 and 16 show the effect of a variation of the initial widths σ_z and σ_y of the species fields c_z and c_y, respectively, for unstratified simulations with $Ri = 0$. Compared to the simulations from the Richardson number variation discussed above, the initial values of σ_z and σ_y are decreased here. Both σ_z and σ_y increase rapidly as the simulations advance in time. The final values of σ_z and σ_y are each nearly identical at the end of the simulations at $St = 12$.

SUMMARY

In this study, direct numerical simulations have been performed in order to study turbulent dispersion in stably stratified shear flow. A series of simulations was performed in which the Richardson number was varied from $Ri = 0$, corresponding to unstratified shear flow, to $Ri = 0.4$, corresponding to strongly stratified shear flow. The total energy

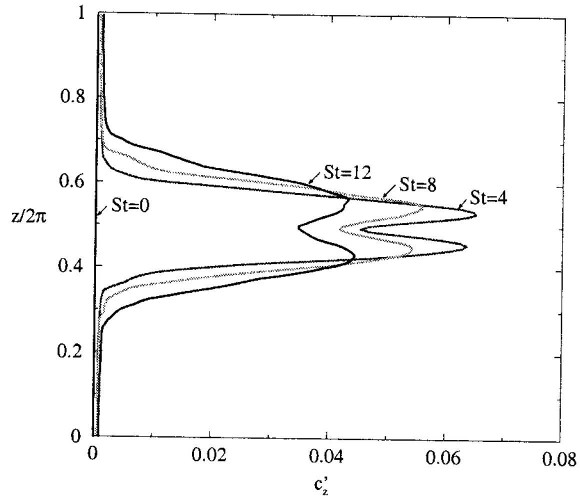

Figure 11: Evolution of the concentration fluctuations c'_z with nondimensional time St. The Richardson number is $Ri = 0.0$.

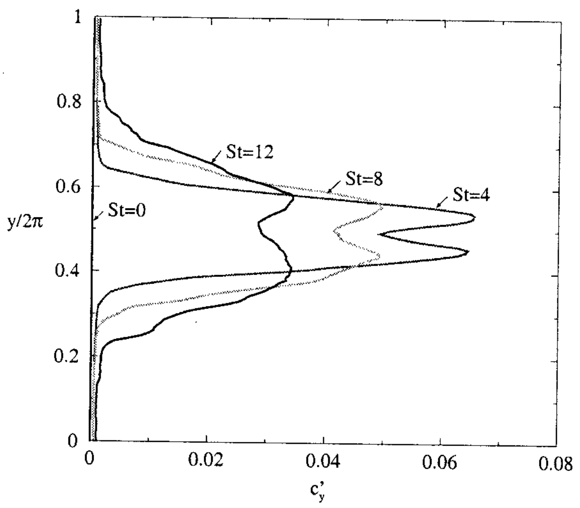

Figure 12: Evolution of the concentration fluctuations c'_y with nondimensional time St. The Richardson number is $Ri = 0.0$.

E was observed to grow for weakly stratified cases with $Ri \leq 0.1$ and to decay for strongly stratified cases with $Ri > 0.1$. The contribution of the kinetic energy to the total energy K/E was found to decrease with increasing Richardson number and the contribution of the potential energy to the total energy K_ρ/E was found to increase with increasing Richardson number. The kinetic energy was distributed over the velocity components with *downstream > spanwise > vertical.*

The dispersion of two species fields c_z and c_y with an initially Gaussian mean concentration variation in the vertical z direction and spanwise y direction, respectively, were considered. Vertical spreading σ_z was found to be weaker that spanwise spreading σ_y for both unstratified and stratified simulations. This is consistent with the observation of a lower turbulent fluctuation level in the vertical velocity component compared to the spanwise velocity component. With increasing Richardson number Ri, the increase of both σ_z and σ_y slows, due to decreasing turbulent velocity fluctuations. A variation of the initial width of the concentration fields resulted in nearly identical final values of both σ_z and

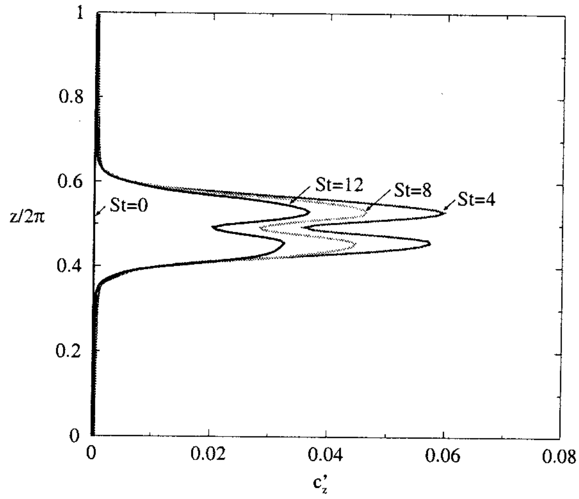

Figure 13: Evolution of the concentration fluctuations c'_z with nondimensional time St. The Richardson number is $Ri = 0.2$.

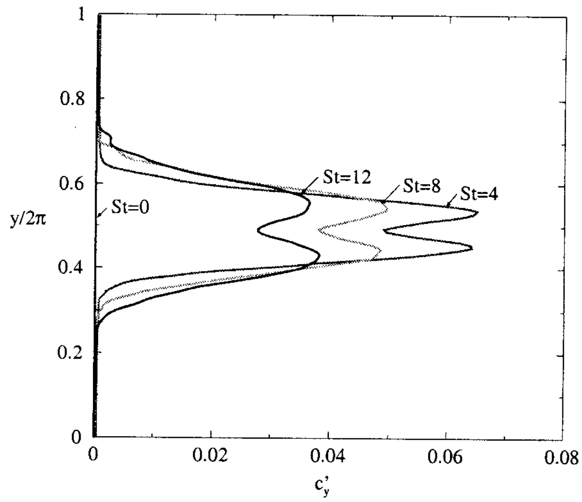

Figure 14: Evolution of the concentration fluctuations c'_y with nondimensional time St. The Richardson number is $Ri = 0.2$.

σ_y at the end of the simulations.

ACKNOWLEDGMENTS

I would like to thank Akula Venkatram for many useful discussions. The simulations have been performed on the parallel computer Lupin at the Institute of Geophysics and Planetary Physics at the University of California, Riverside.

REFERENCES

Gerz, T., Schumann, U., and Elghobashi, S.E., 1989, "Direct numerical simulation of stratified homogeneous turbulent shear flows", *J. Fluid Mech.*, Vol. 200, pp. 563–594.

Holt, S.E., Koseff, J.R., and Ferziger, J.H., 1992, "A numerical study of the evolution and structure of homogeneous stably stratified sheared turbulence", *J. Fluid Mech.*, Vol. 237, pp. 499–539.

Howard, L.N., 1961, "Note on a paper of John W. Miles", *J. Fluid Mech.*, Vol. 10, 509–512.

Hunt, J.C.R., 1982, "Diffusion in the stable boundary layer", In *Atmospheric Turbulence and Air Pollution Mod-*

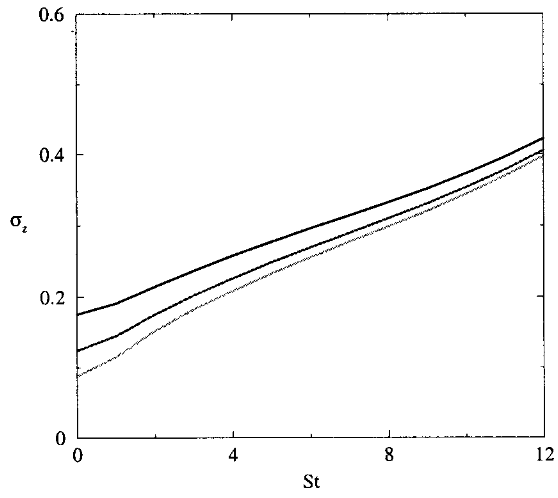

Figure 15: Evolution of the width σ_z with nondimensional time St. The initial width is varied and the Richardson number is $Ri = 0$.

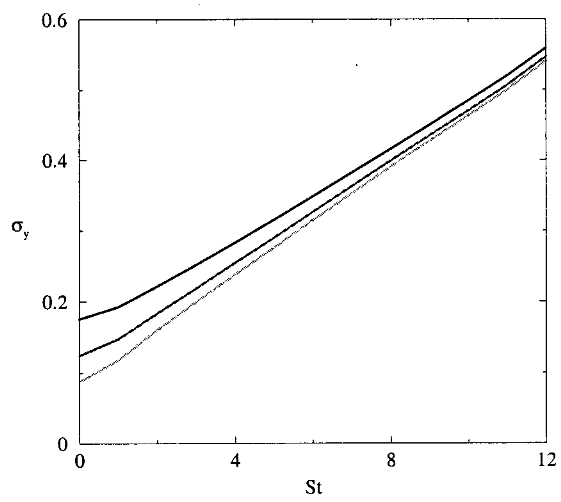

Figure 16: Evolution of the width σ_y with nondimensional time St. The initial width is varied and the Richardson number is $Ri = 0$.

eling. D. Reidel Publishing Company, Dordrecht, Holland, pp. 231–274.

Itsweire, E.C., Koseff, J.R., Briggs, D.A., and Ferziger, J.H., 1993, "Turbulence in stratified shear flows: Implications for interpreting shear-induced mixing in the ocean", *J. Phys. Oceanogr.*, Vol. 23, pp. 1508–1522.

Jacobitz, F.G., Sarkar, S., and Van Atta, C.W., 1997, "Direct numerical simulations of the turbulence evolution in a uniformly sheared and stably stratified flow", *J. Fluid Mech.*, Vol. 342, pp. 231–261.

Jacobitz, F.G., 2000, "Scalar transport and mixing in turbulent stratified shear flow", *Int. J. Heat Fluid Flow*, Vol. 21, pp. 535-541.

Kaltenbach, H.-J., Gerz, T., and Schumann, U., 1994, "Large-eddy simulation of homogeneous turbulence and diffusion in stably stratified shear flow", *J. Fluid Mech.*, Vol. 280, pp. 1–40.

Komori, S., Ueda, H., Ogino, F., and Mizushina, T.,1983, "Turbulence structure in stably stratified open-channel flow", *J. Fluid Mech.*, Vol. 130, pp. 13–26.

Miles, J.W., 1961, "On the stability of heterogeneous shear flows", *J. Fluid Mech.*, Vol. 10, 496–508.

Piccirillo, P.S., and Van Atta, C.W., 1997, "The evolution of a uniformly sheared thermally stratified turbulent flow", *J. Fluid Mech.*, Vol. 334, pp. 61–86.

Richardson, L.F., 1920, "The supply of energy from and to atmospheric eddies", *Proc. Roy. Soc. A*, Vol. 97, 354–373.

Rogallo, R.S., 1981, "Numerical experiments in homogeneous turbulence", *NASA TM 81315*.

Rohr, J.J., Itsweire, E.C., Helland, K.N., and Van Atta, C.W., 1988, "Growth and decay of turbulence in a stably stratified shear flow", *J. Fluid Mech.*, Vol. 195, pp. 77–111.

Taylor, G.I., 1931, "Effect of variation in density on the stability of superposed streams of fluid", *Proc. Roy. Soc. A*, Vol. 132, 499–523.

Venkatram, A., Strimaitis, D., and Dicristofaro, D., 1984, "A semi-empirical model to estimate vertical dispersion of elevated releases in the stable boundary layer", *Atmos. Environ.*, Vol. 18, pp. 923–928.